ORIGINAL RESEARCH

Current-Step Technique to Enhance Plasma Focus Compression and Neutron Yield

S. Lee · S. H. Saw

Abstract A current-step technique is applied to the plasma focus by modifying the Lee Model code, incorporating a current-step bank to add current to the focus pinch at the time of the current dip. For a 50 kV, 1 MJ, 6 μs rise-time bank, the current-step from a 200 kV, 0.4 MJ, 0.8 μs rise-time bank maintains the pinch current at 2.2 MA, enhances compression by 1.9 and increases the neutron yield from 2.5×10^{12} to 1.03×10^{13}. The increase is attributed mainly to the step nature of the current which favorably shifts the end-point of compression; rather than to the scaling in terms of energy or current.

Keywords Current-step plasma focus · Plasma focus modeling · Focus pinch compression enhancement · Neutron enhancement technique · Plasma focus new technology

Introduction

The concept of using energy balance and pressure balance to define the endpoint of a pinch compression was introduced in 1983 [1]. The procedure when applied to an argon pinch produced numerical results in agreement with experiments [2]. Based on the same considerations a current-stepping technique to enhance pinch compressions was suggested in 1984 [3]. The step nature of the current applied just before the end-point of compression favorably shifts the end-point to one of higher compression. Computations showed that such a current-step enables the pinch to be driven to a smaller radius ratio than without the current-step. A current-step pinch was built to demonstrate this effect [4, 5]. The conceptual work was generalized to show that a plasma sphere radially compressed by radiation also attains a smaller radius when the compression is provided in two steps rather than by a single pulse [6]. We now apply this concept to a plasma focus.

In the operation of a plasma focus [7] a capacitor discharge current is used to drive a current sheet down a coaxial tube. At the end of this axial phase the current sheet then sweeps around the central electrode, the anode, accelerating radially until a pinch is formed on-axis. The axial phase serves to delay the radial collapse until the current has reached peak value so that the compression and the pinch occur near the peak current. Typically for a large focus the current rise-time takes several microseconds flattening towards the top like a damped and distorted sinusoidal waveform followed by a relatively sharp (hundreds of ns) dip in the current as the energy is pumped from the magnetic field to strongly compress and heat the plasma.

In an efficient device such as the PF1000 the current is dropped by almost 40% (see Fig. 1) [8]. It is surmised that at this time of current dip it may be beneficial if an additional current is provided so that the current driving the compression and pinch is not reduced so drastically. Moreover according to energy balance and pressure balance described in earlier work the end-point of compression is shifted to a smaller radius by such a current-step. These balances of energy and pressure are implicit in any correctly formulated numerical scheme. We now model

S. Lee · S. H. Saw
INTI International University, 71800 Nilai, Malaysia

S. H. Saw
e-mail: sorheoh.saw@newinti.edu.my

S. Lee (✉) · S. H. Saw
Institute for Plasma Focus Studies, 32 Oakpark Drive, Chadstone, VIC 3148, Australia
e-mail: leesing@optusnet.com.au
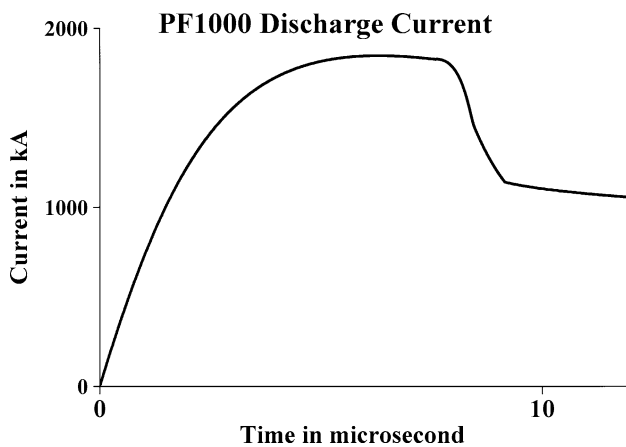
Fig. 1 PF1000 discharge current computed and fitted to measured current [8]. The axial phase ends at 7.6 μs and the current starts dipping at 7.9 μs at 1,800 kA dropping to 1,130 kA at 9.3 μs

such an additional current step applied to the plasma focus. We start with the basic Lee Model code briefly discussed in the next paragraphs.

The Lee model code couples the electrical circuit with plasma focus dynamics, thermodynamics and radiation, enabling realistic simulation of all gross focus properties. The basic model, described in 1984 [9] was successfully used to assist several projects [10–14]. Radiation-coupled dynamics was included in the five-phase code leading to numerical experiments on radiation cooling [13]. The vital role of a finite small disturbance speed discussed by Potter in a Z-pinch situation [15] was incorporated together with real gas thermodynamics and radiation-yield terms. This version of the code assisted other research projects [16–24] and was web-published in 2000 [25]. Plasma self-absorption was included in 2007 [25] improving SXR yield simulation [26–31]. The code has been used extensively in several machines including UNU/ICTP PFF [10, 13, 14, 16, 18–24, 31–35], NX2 [17, 18, 36], NX1 [18, 34, 37], and adapted for the Filippov-type plasma focus DENA [38]. A recent development is the inclusion of the neutron yield, Y_n, using a beam–target mechanism [8], incorporated in recent versions [39] of the code (versions later than RADPFV5.13), resulting in realistic Y_n scaling with I_{pinch} [40–43]. The versatility and utility of the model is demonstrated in its clear distinction of I_{pinch} from I_{peak} [44] and the recent uncovering of a plasma focus pinch current limitation effect [45, 46]. The description, theory, code and a broad range of results of this 'Universal Plasma Focus Laboratory Facility' is available for download from [39, 47].

A brief description of the code is given below. The five phases are summarised as follows with the description modified to include the current-step circuit:

1. Axial phase: Described by a snowplow model with an equation of motion which is coupled to two circuit equations accounting for the two capacitor banks. The equation of motion incorporates the axial phase model parameters: mass and current factors f_m and f_c [11, 48, 49]. The mass swept-up factor f_m accounts for not only the porosity of the current sheet but also for the inclination of the moving current sheet-shock front structure and all other unspecified effects which have effects equivalent to increasing or reducing the amount of mass in the moving structure [49–51] during the axial phase. The current factor, f_c, accounts for the fraction of current effectively flowing in the moving structure (due to all effects such as current shedding at or near the back-wall, current sheet inclination). This defines the fraction of current effectively driving the structure, during the axial phase.

2. Radial inward shock phase: Described by five coupled equations using an elongating slug model. The first equation computes the radial inward shock speed from the driving magnetic pressure. The second equation computes the axial elongation speed of the column. The third equation computes the speed of the current sheath, also called the magnetic piston, allowing the current sheath to separate from the shock front by applying an adiabatic approximation. The fourth and fifth are the circuit equations of the two capacitor banks. Thermodynamic effects due to ionization and excitation are incorporated into these equations, these effects being important for gases other than hydrogen and deuterium. Temperature and number densities are computed during this phase. A communication delay between shock front and current sheath due to the finite small disturbance speed is crucially implemented in this phase. The model parameters, radial phase mass swept-up and current factors, f_{mr} and f_{cr}, are incorporated in all three radial phases. The mass swept-up factor f_{mr} accounts for all mechanisms which have effects equivalent to increasing or reducing the amount of mass in the moving slug, during the radial phase. The current factor, f_{cr}, accounts for the fraction of current effectively flowing in the moving piston forming the back of the slug (due to all effects). This defines the fraction of current effectively driving the radial slug.

3. Radial reflected shock (RS) phase: When the shock front hits the axis, because the focus plasma is collisional, a reflected shock develops which moves radially outwards, whilst the radial current sheath piston continues to move inwards. Five coupled equations are also used to describe this phase, these being for the reflected shock moving radially outwards, the piston moving radially inwards, the elongation of the annular column and the two circuit equations. The same model parameters, f_{mr} and f_{cr}, are used as in the previous radial phase. The

plasma temperature behind the reflected shock undergoes a jump by a factor nearly 2.

4. Slow compression (quiescent) or pinch phase: When the out-going reflected shock hits the in-going piston the compression enters a radiative phase in which for gases such as neon, radiation emission may actually enhance the compression where we have included energy loss/gain terms from Joule heating and radiation losses into the piston equation of motion. Four coupled equations describe this phase; these being the piston radial motion equation, the pinch column elongation equation and the two circuit equations, incorporating the same model parameters as in the previous two phases. Thermodynamic effects are incorporated into this phase. The duration of this slow compression phase is set as the time of transit of small disturbances across the pinched plasma column. The computation of this phase is terminated at the end of this duration.

5. Anomalous resistance phase and expanded column phase: To simulate the current trace beyond this point we allow the column to suddenly attain the radius of the anode, and use the expanded column inductance for further integration. For simplicity we have not included the anomalous resistance phase [52] into this current-step modelling. This will be considered in a later project.

Theory

Two capacitor banks, in parallel, are connected to a plasma focus tube (Fig. 2). The first capacitor bank, C_1, L_1, r_1 is switched onto the plasma focus at time $t = 0$. The second capacitor bank, C_2, L_2, r_2, is switched after an interval of
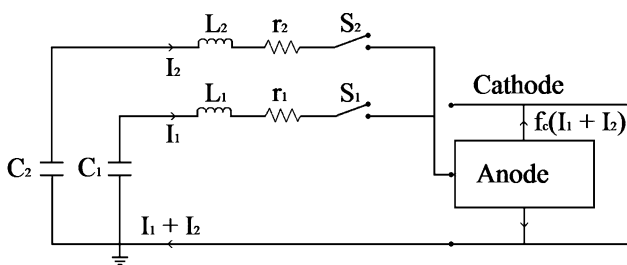
Fig. 2 Schematic of the current-stepped PF. The main bank with components C_1, L_1 and r_1 is switched by S_1 onto the anode, with mesh current I_1. The current taking part in the plasma dynamics is $f_c I_1$ with $(1 - f_c)I_1$ being a leakage current. Just before peak I_1, the current-step bank with C_2, L_2 and r_2 is switched by S_2 onto the anode, with mesh current I_2. The total current flowing into the anode is $I = I_1 + I_2$. The current taking part in the plasma dynamics is $f_c(I_1 + I_2)$; shown in this figure flowing in the axial phase. The leakage path of remnant current $(1 - f_c)(I_1 + I_2)$ is not shown

time t_s. Time of switching, t_s is distance controlled. For example t_s may be the time when the current sheet has reached say 0.9 of the axial phase; i.e., when $z = 0.9z_0$; or t_s may be the time after the end of the axial phase, when the current sheet has reached say 0.7 of the anode radius i.e., when $r_p = 0.7a$. In either case it is readily seen that in order for the current step to be effective, its rise-time must be shorter than the rise-time of the first capacitor bank.

Axial Phase

This phase is characterized by the linearly (with axial distance) increasing nature of the tube inductance $L = \frac{\mu}{2\pi} \ln(b/a)z(t)$ as the current sheet moves down the tube carrying a fraction f_c of the capacitor discharge current.

Hence $\quad \dfrac{dL}{dt} = \dfrac{L_a}{z_0} \dfrac{dz}{dt} \quad$ where $L_a = \dfrac{\mu}{2\pi} \ln \dfrac{b}{a} z_0$.

The current $f_c(I_1 + I_2)$ drives the plasma sheath to a speed dz/dt. Using a modified snowplow model assuming fraction f_m of the encountered mass is swept up, the equation of motion may be written as: (with $C = b/a$)

$$\frac{d^2z}{dt^2} = \frac{\left[\frac{f_c^2}{f_m} \frac{L_a}{z_0 2\pi \rho_0 (C^2-1)} \left(\frac{I_1+I_2}{a}\right)^2 - \left(\frac{dz}{dt}\right)^2\right]}{z} \tag{1}$$

The equation governing the first capacitor bank is written down using mesh $C_1 - L_1 - r_1 - L_p$:

$$\frac{dI_1}{dt} = \frac{\left[V_1 - \frac{\int I_1 dt}{C_1} - \frac{L_a}{z_0} f_c(I_1+I_2)\frac{dz}{dt} - \frac{L_a}{z_0} f_c z \frac{dI_2}{dt} - r_1 I_1\right]}{\left[L_1 + f_c \frac{L_a}{z_0}\right]} \tag{2}$$

The equation governing the second capacitor bank is written down using the mesh $C_2 - L_2 - r_2 - L_p$:

$$\frac{dI_2}{dt} = \frac{\left[V_2 - \frac{\int I_2 dt}{C_2} - \frac{L_a}{z_0} f_c(I_1+I_2)\frac{dz}{dt} - \frac{L_a}{z_0} f_c z \frac{dI_1}{dt} - r_2 I_2\right]}{\left[L_2 + f_c \frac{L_a}{z_0} z\right]} \tag{3}$$

During the axial phase these three equations (1)–(3) are the generating equations, coupled together to solve the three unknowns I_1, I_2 and z.

However before the second capacitor bank is switched on, $I_2 = 0$, $dI_2/dt = 0$; and effectively only two equations operate namely that governing the first capacitor bank and the axial equation of motion.

An additional useful equation may be written for the tube voltage as:

$$V = \frac{d}{dt}(LIf_c) = \frac{L_a}{z_0} f_c(I_1+I_2)\frac{dz}{dt} + f_c \frac{L_a}{z_0} z \left(\frac{dI_1}{dt} + \frac{dI_2}{dt}\right) \tag{4}$$

Radial Phase

$$\frac{dr_s}{dt} = -\left(\frac{\mu(\gamma+1)}{\rho_0}\right)^{1/2}\frac{f_{cr}}{\sqrt{f_{mr}}}\frac{(I_1+I_2)}{4\pi r_p} \tag{5}$$

$$\frac{dz_f}{dt} = -\left(\frac{2}{\gamma+1}\right)\frac{dr_s}{dt} \tag{6}$$

Reflected Shock Phase

$$\text{Reflected shock speed} = -0.3\left(\frac{dr_s}{dt}\right)_{\text{on–axis}} \tag{11}$$

Piston speed:

$$\frac{dr_s}{dt} = \frac{\frac{2}{\gamma+1}\frac{r_s}{r_p}\frac{dr_s}{dt} - \frac{r_p}{\gamma(I_1+I_2)}\left(1-\frac{r_s^2}{r_p^2}\right)\left(\frac{dI_1}{dt}+\frac{dI_2}{dt}\right) - \frac{1}{\gamma+1}\frac{r_p}{z_p}\left(1-\frac{r_s^2}{r_p}\right)\frac{dz_f}{dt}}{\frac{\gamma-1}{\gamma}+\frac{1}{\gamma}\frac{r_s^2}{r_p^2}} \tag{12}$$

$$\frac{dr_p}{dt} = \frac{\left[\left(\frac{2}{\gamma+1}\right)\frac{r_s}{r_p}\frac{dr_s}{dt} - \left(1-\left(\frac{r_s}{r_p}\right)^2\right)\left(\frac{dI_1}{dt}+\frac{dI_2}{dt}\right) - \left(\frac{1}{\gamma+1}\right)\left(\frac{r_p}{z_f}\right)\left(1-\left(\frac{r_s}{r_p}\right)^2\right)\frac{dz_f}{dt}\right]}{\left[\frac{\gamma-1}{\gamma}+\frac{1}{\gamma}\left(\frac{r_s}{r_p}\right)^2\right]} \tag{7}$$

where we are reminded: r_p = radial piston position, r_s = radial shock front position, z_f = axial piston position

Column elongation speed: $\frac{dz_f}{dt} = -\left(\frac{2}{\gamma+1}\right)\left(\frac{dr_s}{dt}\right)_{\text{on–axis}} \tag{13}$

$$\frac{dI_1}{dt} = \frac{V_1 - \frac{\int I_1 dt}{C_1} - r_1 I_1 - f_{cr}L_a\left(1+\frac{z_f\ln(b/r_p)}{z_0\ln C}\right)\frac{dI_2}{dt} - \frac{f_{cr}L_a(I_1+I_2)}{z_0\ln C}\left(\ln(b/r_p)\frac{dz_f}{dt}-\frac{z_f}{r_p}\frac{dr_p}{dt}\right)}{L_1+f_{cr}L_a\left(1+\frac{z_f}{z_0}\frac{\ln(b/r_p)}{\ln C}\right)} \tag{8}$$

$$\frac{dI_2}{dt} = \frac{V_2 - \frac{\int I_2 dt}{C_2} - r_2 I_2 - f_{cr}L_a\left(1+\frac{z_f\ln(b/r_p)}{z_0\ln C}\right)\frac{dI_1}{dt} - \frac{f_{cr}L_a(I_1+I_2)}{z_0\ln C}\left(\ln(b/r_p)\frac{dz_f}{dt}-\frac{z_f}{r_p}\frac{dr_p}{dt}\right)}{L_2+f_{cr}L_a\left(1+\frac{z_f}{z_0}\frac{\ln(b/r_p)}{\ln C}\right)} \tag{9}$$

During the radial phase these five equations (5)–(9) are the generating equations, coupled together to solve step-by-step the five unknowns I_1, I_2 and z_f, r_p and r_s.

The tube voltage across the PF is calculated using the following equation:

$$V = f_{cr}\frac{L_a}{z_0\ln C}\left[z_0\ln C + \ln(b/r_p)z_f\right]\left[\frac{dI_1}{dt}+\frac{dI_2}{dt}\right] + \left[\ln(b/r_p)\frac{dz_f}{dt}-\frac{z_f}{r_p}\frac{dr_p}{dt}\right][I_1+I_2] \tag{10}$$

A signal communication time correction is applied in this phase by coupling the small disturbances speed.

To compute $\frac{dI_1}{dt}$ and $\frac{dI_2}{dt}$ we use (8) and (9).

Equations (8), (9), and (11)–(13) are the five generating equations for this phase which are coupled. These are solved simultaneously by a step-by-step method for the five unknowns I_1, I_2, z_f, r_p and the reflected shock speed with $r_s = 0$.

The tube voltage equation is (10) except put $\left(\frac{dr_s}{dt}\right) = 0$.

When the radially out-going RS hits the 'magnetic piston' r_p, the RS phase ends and the computation moves to the slow compression or pinch phase.

Pinch Phase

In the slow compression or pinch phase we have a very dense hot plasma where the radiation loss from the plasma may affect the dynamics and when the loss is severe enough may lead to radiation collapse. This effect is however opposed by the Joule heating term which heats the plasma and tends to increase the radius of the confined plasma. To allow for the interaction of the energy gain/loss term Q with the dynamics of the column we couple Q to the dynamics and obtain the following equation governing the boundary r_p of the column:

$$\frac{dr_p}{dt} = \frac{\frac{-r_p}{\gamma I}\frac{dI}{dt} - \frac{1}{\gamma+1}\frac{r_p}{z_f}\frac{dz_f}{dt} + \frac{4\pi(\gamma-1)}{\mu\gamma z_f}\frac{r_p}{f_c^2 I^2}\frac{dQ}{dt}}{\frac{\gamma-1}{\gamma}} \qquad (14)$$

where we have written $I = I_1 + I_2$.

Column elongation   We also compute the elongation of the column as being driven fully by the plasma pressure:

$$\frac{dz_f}{dt} = \left[\frac{\mu}{4\pi^2(\gamma+1)\rho_o}\right]^{1/2}\frac{If_c}{r_p} \qquad (15)$$

The four equations (8), (9), (14) and (15) are considered as the generating equations for this phase, coupled together and are solved step-by-step for the four unknowns $I_1, I_2, z_f,$ and r_p.

Together with the following equations needed to determine Q at each point.

To compute the Joule heating we use: (with Z = effective charge number)

$$\frac{dQ_J}{dt} = R(I_1 + I_2)^2 f_{cr}^2 \quad \text{where } R = \frac{1290 Z z_f}{\pi r_p^2 T^{3/2}}$$

$$T = \frac{\mu}{8\pi^2 k}(I_1 + I_2)^2 f_c^2 / ((1 + Z)N_0 a^2 f_{mr})$$

To compute the radiation loss we include Bremsstrahlung and line as follows:

The Bremsstrahlung loss term is written as:

$$\frac{dQ_B}{dt} = -1.6 \times 10^{-40} N_i^2 \left(\pi r_p^2\right) z_f T^{1/2} z^3$$

$$N_0 = 6 \times 10^{26}\frac{\rho_0}{M}; \quad N_i = N_a f_{mr}\left(\frac{a}{r_p}\right)^2$$

where M = molecular weight and ρ_0 = ambient density.

The line radiation loss term may be written as:

$$\frac{dQ_L}{dt} = -4.6 \times 10^{-31} N_i^2 Z Z_n^4 \left(\pi r_p^2\right) z_f / T$$

where Z_n = atomic number, and

$$\frac{dQ}{dt} = \frac{dQ_J}{dt} + \frac{dQ_B}{dt} + \frac{dQ_L}{dt}$$

where $\frac{dQ}{dt}$ is the total power gain/loss of the plasma column.

By this coupling, if, for example, the radiation loss $\left(\frac{dQ_B}{dt} + \frac{dQ_L}{dt}\right)$ is severe, this would lead to a large value of $\frac{dr_p}{dt}$

inwards. In the extreme case, this leads to radiation collapse, with r_p going rapidly to zero, or to such small values that the plasma becomes opaque to the outgoing radiation, thus stopping the radiation loss.

This radiation collapse occurs at a critical current of 1.6 MA (the Pease–Braginski current) for deuterium. For gases such as Neon or Argon, because of intense line radiation, the critical current is reduced to even below 100 kA, depending on the plasma temperature. Plasma self absorption is also included.

For the tube voltage we continue to use (10).

The Results

This code was based on the 5-phase code version 5.15d [39] but terminated at the end of the pinch phase. To show the effect of current-stepping we choose a MJ bank which was designed and optimized in a previous exercise [41].

Capacitor Bank 1 (0.97 MJ)

$L_0 = 36$ nH, $C_0 = 777$ μF, $V_0 = 50$ kV, $r_0 = 0.83$ mΩ matched to the following PF tube combination: $b = 23.44$ cm, $a = 16.86$ cm, $z_0 = 35$ cm operated at $P_0 = 10$ Torr with the following model parameters: $f_m = 0.13, f_c = 0.65, f_{mr} = 0.35$ and $f_{cr} = 0.65$.

Capacitor Bank 2 (the Current-Stepping Bank, 0.4 MJ)

$L_0 = 10$ nH, $C_0 = 20$ μF, $V_0 = 200$ kV, $r_0 = 2.2$ mΩ stepped at time during the radial phase when the piston has reached $r_p = 0.34$ i.e., close to the maximum compression.

The choice of this combination is based on the following considerations. From earlier work it was decided not to go to too high a voltage for the main bank since in the beam target model at operating voltage of 50 kV, the effective beam energy is close to 150 keV where the D–D fusion cross section with energy curve is already flattening and no longer gaining much with further increase in beam energy. For the second bank we tested various combinations and eventually found a reasonably effective one using the lowest practicable inductance of 10 nH. This bank has a rise-time of 0.8 μs which is found to be effective for the radial phase duration of just over 2 μs. Tests include choosing the value of C_2 then moving the switching time looking for optimum Y_n.

The results are shown in Fig. 3. When the main bank is fired without switching the current-step bank, the current is seen to dip strongly (from just past 6 μs to just past 8 μs as shown in curve labeled 'I_1'). The Y_n is 2.5×10^{12}. When the current-step bank is switched on at $r_p = 0.34a$ its current
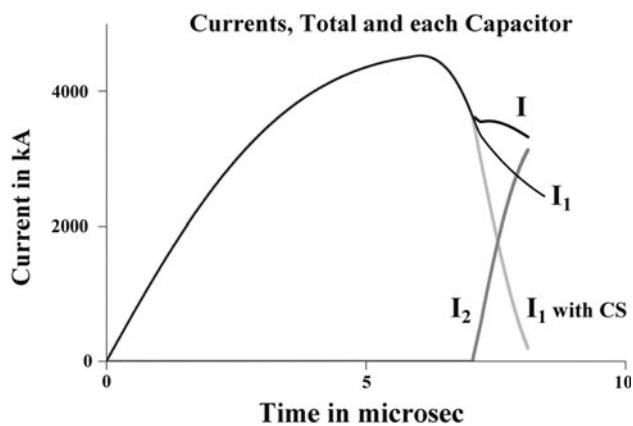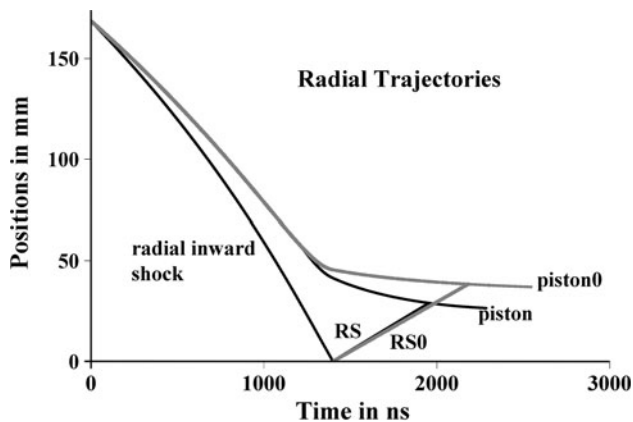
Fig. 3 Comparing the current waveforms of main bank (I_1 with CS), current-step bank (I_2) and the combined current (I). Also shown for comparison is the current when the current-step is not switched on (I_1)

'I_2' is displayed. The result of switching the current-step bank is that the main bank current labeled 'I_1 with CS' is seen to drop faster as a result of part of the current from the current-step bank flowing into the main bank. Nevertheless the total current $I = I_1 + I_2$ entering the PF is increased. For this current-step configuration the switch timing is not critical with a range of switching from $r_p = 0.33a$ to $r_p = 0.43a$ producing optimum Y_n at 1.03×10^{13}.

The effect of the current-step is most marked on the radial trajectory of the current sheet (piston) after the switching of the current-step (see Fig. 4). Without switching the current-step (see curve 'piston0'), minimum pinch radius r_{min} reaches 36.8 mm whilst with the current-step (see curve 'piston') the pinch compression is more severe, r_{min} reaching 27 mm. The pinch density is increased by 1.9 times. This increase in compression contributes to the increase in Y_n.

Summarizing, the main bank (0.97 MJ) had been optimized to yield D–D neutrons per shot of 2.5×10^{12}. With the addition of the current-step bank of energy (0.4 MJ) Y_n is boosted by a factor of 4 to 1.03×10^{13}. The current-step

is switched on 0.8 μs before the start of the pinch which has a duration of 320 ns. The increase in pinch current I_{pinch} is maintained throughout the period of the pinch. Without current-step, I_{pinch} dropped from 1.7 to 1.6 MA; whilst with current-step I_{pinch} is still at a level of 2.2 MA at the end of the pinch. A study of the scaling laws [40, 41, 50, 51] shows that the increase in Y_n is significantly beyond the scaling according to energy or currents. Hence it may be concluded that the step nature of the current [3–5] is largely responsible for the significantly enhanced Y_n as predicted by the favorable shift of the endpoint of the pinch due to the current-step.

Conclusion

The concept of using energy balance and pressure balance to define the end-point of a pinch predicts that a step-current shifts the final pinch radius to a smaller value thus enhancing compression and neutron yield. This concept is applied to the plasma focus with the implementation of a current-stepping circuit onto the Lee Model code. For a 50 kV, 1 MJ, 6 μs rise-time bank, the current-step from a 200 kV, 0.4 MJ, 0.8 μs rise-time bank maintains the pinch current at 2.2 MA, enhances compression by 1.9 and increases the neutron yield by a factor of 4 from 2.5×10^{12} to 1.03×10^{13}. The increase is attributed mainly to the step nature of the current which favorably shifts the end-point of compression; rather than to the scaling in terms of energy or current. The current-step technique may be useful to compensate for the deterioration [42, 50, 51] of Y_n scaling law with energy. This may be useful for scaling up the plasma focus for fusion energy applications and for fusion-reactor related materials studies [8, 53, 54].

Fig. 4 Comparing radial trajectories with and without current step

References

1. S. Lee, An energy-consistent snow-plough model for pinch design. J. Phys. D Appl. Phys. **16**, 2463–2469 (1983)
2. S. Lee, Radius ratios of argon pinches. Aust. J. Phys. **36**, 891–895 (1983)
3. S. Lee, A current-stepping technique to enhance pinch compression. J. Phys. D Appl. Phys. **17**, 733–739 (1984)
4. S.H. Saw, S. Lee, C.S. Wong, in *A Current-Stepping Technique to Enhance Pinch Compression—an Experimental Study in Small Plasma Physics Experiments (II)*, ed. by S. Lee, P.H. Sakanaka (World Scientific, Singapore, 1990), pp. 289–295, ISBN 981-02-0285-7
5. S.H. Saw, *Experimental Studies of a Current-Stepped Pinch*. PhD Thesis, Universiti Malaya, Malaysia, 1990
6. S. Lee, Density ratios in compressions driven by radiation pressure. Laser Part. Beams **6**, 597–606 (1988)
7. A. Bernard, H. Bruzzone, P. Choi, H. Chuaqui, V. Gribkov, J. Herrera, K. Hirano, A. Krejci, S. Lee, C. Luo, F. Mezzetti, M.

Sadowski, H. Schmidt, K. Ware, C.S. Wong, V. Zoita, Scientific status of plasma focus research. Mosc. J. Phys. Soc. **8**, 93–170 (1998)

8. V.A. Gribkov, A. Banaszak, B. Bienkowska, A.V. Dubrovsky, I. Ivanova-Stanik, L. Jakubowski, L. Karpinski, R.A. Miklaszewski, M. Paduch, M. Sadowski, M. Scholz, A. Szydlowski, K. Tomaszewski, Plasma dynamics in the PF-1000 device under full scale energy storage: II. Fast electron and ion characteristics versus neutron emission parameters and gun optimization perspectives. J. Phys. D Appl. Phys. **40**(12), 3592–3607 (2007)

9. S. Lee, Plasma focus model yielding trajectory and structure, in *Radiations in Plasmas*, vol. II, ed. by B. McNamara (World Scientific, Singapore, 1984), pp. 978–987

10. S. Lee, T.Y. Tou, S.P. Moo, M.A. Eissa, A.V. Gholap, K.H. Kwek, S. Mulyodrono, A.J. Smith, S. Suryadi, W. Usada, M. Zakaullah, A simple facility for the teaching of plasma dynamics and plasma nuclear fusion. Am. J. Phys. **56**(1), 62–68 (1988)

11. T.Y. Tou, S. Lee, K.H. Kwek, Non perturbing plasma focus measurements in the run-down phase. IEEE Trans. Plasma Sci. **17**(2), 311–315 (1989)

12. S. Lee, A sequential plasma focus. IEEE Trans. Plasma Sci. **19**(5), 912–919 (1991)

13. J. Ali, *Development and studies of a small plasma focus*. Ph.D. Dissertation, Universiti Teknologi Malaysia, Malaysia, 1990

14. S.P. Moo, C.K. Chakrabarty, S. Lee, An investigation of the ion beam of a plasma focus using a metal obstacle and a deuterated target. IEEE Trans. Plasma Sci. **19**, 515–519 (1991)

15. D.E. Potter, The formation of high-density z-pinches. Nucl. Fusion **18**, 813–823 (1978)

16. M. Liu, *Soft X-Rays from Compact Plasma Focus*. Ph.D. dissertation, NIE, Nanyang Technological Univ., Singapore, 2006. ICTP Open Access Archive [online]. Available: http://eprints.ictp.it/327/

17. S. Bing, *Plasma Dynamics and X-Ray Emission of the Plasma Focus*. Ph.D. dissertation, NIE, Nanyang Technological Univ., Singapore, 2000. ICTP Open Access Archive [online]. Available: http://eprints.ictp.it/99/

18. G. Zhang, *Plasma Soft X-Ray Source for Microelectronics Lithography*. PhD dissertation, NIE, Nanyang Technological Univ Singapore, 1999

19. A. Serban, S. Lee, Experiments on speed-enhanced neutron yield from a small plasma focus. J. Plasma Phys. **60**(1, pt. 1), 3–15 (1998)

20. M.H. Liu, X.P. Feng, S.V. Springham, S. Lee, Soft X-ray measurement in a small plasma focus operated in neon. IEEE Trans. Plasma Sci. **26**(2), 135–140 (1998)

21. S. Lee in *Twelve Years of UNU/ICTP PFF—a Review* (Abdus Salam ICTP, Trieste, 1998), pp. 5–34. IC/98/231, ICTP Open Access Archive [online]. Available: http://eprints.ictp.it/31/

22. S. Lee, A. Serban, Dimensions and lifetime of the plasma focus pinch. IEEE Trans. Plasma Sci. **24**(3), 1101–1105 (1996)

23. S. Lee, *Scaling of the Plasma Focus-Viewpoint from Dynamics*. International Plasma Focus Symposium, Kudowa, July 1998

24. S. Lee, Characterising the plasma focus pinch and speed enhancing the neutron yield. In *First Cairo Conference on Plasma Physics & Applications, 11–15 Oct 2004*. International Cooperation Bilateral Seminars (vol. 34). Forschungszentrum Juelich GmbH, Juelich, pp. 27–33. ISBN 3-89336-374-2

25. S. Lee, [online]. Radiative dense plasma focus computation package: RADPF (2011). Available: http://ckplee.home.nie.edu.sg/plasmaphysics/

26. M. Akel, S. Al-Hawat, S. Lee, Pinch current and soft X-ray yield limitation by numerical experiments on nitrogen plasma focus. J. Fusion Energ. **29**, 94–99 (2010)

27. S. Lee, S.H. Saw, P. Lee, R.S. Rawat, Numerical experiments on neon plasma focus soft X-rays scaling. Plasma Phys. Control. Fusion, **51**, 105013 (8 pp) (2009)

28. M. Akel, S. Al-Hawat, S. Lee, Numerical experiments on soft X-ray emission optimization of nitrogen plasma in 3 KJ plasma focus SY-1 using modified lee model. J. Fusion Energ. **28**, 355–363 (2009)

29. M. Akel, S. Al-Hawat, S.H. Saw, S. Lee, Numerical experiments on oxygen soft X-ray emissions from low energy plasma focus using Lee model. J. Fusion Energ. **29**, 223–231 (2010)

30. S. Lee, P. Lee, R.S. Rawat, S.H. Saw, Soft X-ray yield from NX2 plasma focus. J. Appl. Phys. **106**, 023 309 (2009)

31. S.H. Saw, P.C.K. Lee, R.S. Rawat, S. Lee, Optimizing UNU/ICTP PFF plasma focus for neon soft X-ray operation. IEEE Trans Plasma Sci **37**, 1276–1282 (2009)

32. S.V. Springham, S. Lee, M.S. Rafique, Correlated deuteron energy spectra and neutron yield for a 3 kJ plasma focus. Plasma Phys. Control. Fusion **42**(10), 1023–1032 (2000)

33. M.A. Mohammadi, S. Sobhanian, C.S. Wong, S. Lee, P. Lee, R.S. Rawat, The effect of anode shape on neon soft X-ray emissions and current sheath configuration in plasma focus device. J. Phys. D Appl. Phys. **42**(4), 045 203 (10 pp) (2009)

34. S. Lee, P. Lee, G. Zhang, X. Feng, V.A. Gribkov, M. Liu, A. Serban, T. Wong, High rep rate high performance plasma focus as a powerful radiation source. IEEE Trans. Plasma Sci. **26**(4), 1119–1126 (1998)

35. S.H. Saw, S. Lee, F. Roy, P.L. Chong, V. Vengadeswaran, A.S.M. Sidik, Y.W. Leong, A. Singh, In situ determination of the static inductance and resistance of a plasma focus capacitor bank. Rev. Sci. Instrum. **81**, 053505 (2010)

36. D. Wong, P. Lee, T. Zhang, A. Patran, T.L. Tan, R.S. Rawat, S. Lee, An improved radiative plasma focus model calibrated for neon filled NX2 using a tapered anode. Plasma Sources Sci. Technol. **16**(1), 116–123 (2007)

37. E.P. Bogolyubov, V.D. Bochkov, V.A. Veretennikov, L.T. Vekhoreva, V.A. Gribkov, A.V. Dubrovskii, Y.P. Ivanov, A. Isakov, O.N. Krokhin, P. Lee, S. Lee, V.Y. Nikulin, A. Serban, P.V. Silin, X. Feng, G.X. Zhang, A powerful soft X-ray source for X-ray lithography based on plasma focusing. Phys. Scr. **57**(4), 488–494 (1998)

38. V. Siahpoush, M.A. Tafreshi, S. Sobhanian, S. Khorram, Adaptation of Sing Lee's model to the Filippov type plasma focus geometry. Plasma Phys. Control. Fusion **47**, 1065–1075 (2005)

39. S. Lee, (online) *Radiative Dense Plasma Focus Computation Package: RADPF*, 2011. http://www.plasmafocus.net

40. S. Lee, S.H. Saw, Neutron scaling laws from numerical experiments. J. Fusion Energ. **27**, 292–295 (2008)

41. S. Lee, Current and neutron scaling for Megajoule plasma focus machines. Plasma Phys. Control. Fusion, **50**(10), 105 005 (14 pp) (2008)

42. S. Lee, Neutron yield saturation in plasma focus-a fundamental cause. Appl. Phys. Lett. **95**, 151 503 (published online 15 Oct 2009)

43. S. Lee, S.H. Saw, L. Soto, S.P. Moo, S.V. Springham, Numerical experiments on plasma focus neutron yield versus pressure compared with laboratory experiments. Plasma Phys. Control. Fusion **51**, 075 006 (11 pp) (2009)

44. S. Lee, S.H. Saw, P.C.K. Lee, R.S. Rawat, H. Schmidt, Computing plasma focus pinch current from total current measurement. Appl. Phys. Lett. **92**(11), 111 501 (2008)

45. S. Lee, S.H. Saw, Pinch current limitation effect in plasma focus. Appl. Phys. Lett. **92**(2), 021 503 (2008)

46. S. Lee, P. Lee, S.H. Saw, R.S. Rawat, Numerical experiments on plasma focus pinch current limitation. Plasma Phys. Control. Fusion **50**(6), 065 012 (8 pp) (2008)

47. S. Lee, *Radiative Dense Plasma Focus Computation Package: RADPF*, 2011. http://www.intimal.edu.my/school/fas/UFLF/
48. S.P. Chow, S. Lee, B.C. Tan, Current sheath studies in a co-axial plasma focus gun. J. Plasma Phys. **8**, 21–31 (1972)
49. S. Al-Hawat, M. Akel, S. Lee, S.H. Saw, Model parameters vs gas pressure in two different plasma focus devices operated in Argon and Neon. J. Fusion Energ. **31**, 13–20 (2012)
50. S.H. Saw, S. Lee, Scaling the plasma focus for fusion energy considerations. Int. J. Energy Res. **35**, 81–88 (2011)
51. S.H. Saw, S. Lee, Scaling laws for plasma focus machines from numerical experiments. Energy Power Eng. **1**, 65–72 (2010)
52. S. Lee, S.H. Saw, A.E. Abdou, H. Torreblanca, Characterising plasma focus devices—role of static inductance—instability phase fitted by anomalous resistance. J Fusion Energ. **30**, 277–282 (2011)
53. S. Lee, S.H. Saw, Nuclear fusion energy—mankind's giant step forward. J. Fusion Energ. **30**, 398–403 (2011)
54. S. Lee, S.H. Saw, *Nuclear Fusion Energy—the Role of the Plasma Focus*. Keynote address at International Workshop on Plasma Science and Applications 27–28 Oct 2011, Tehran, Iran